Research Square

Preprints are preliminary reports that have not undergone peer review.
They should not be considered conclusive, used to inform clinical practice,
or referenced by the media as validated information.

Analysis of The Cells Isolated From Epithelial Cell Rests of Malassez Through Single-cell Limiting Dilution

Syed Taufiqul Islam
Health Sciences University of Hokkaido
Yoshihito Kurashige
Health Sciences University of Hokkaido
Dembereldorj Bolortsetseg
Health Sciences University of Hokkaido
Erika Minowa
Health Sciences University of Hokkaido
Yunosuke Okada
Health Sciences University of Hokkaido
Sayaka Sakakibara
Health Sciences University of Hokkaido
Yoshihiro Abiko
Health Sciences University of Hokkaido
Masato Saitoh (msaitoh@hoku-iryo-u.ac.jp)
Health Sciences University of Hokkaido

Research Article

Keywords: Periodontal ligament (PDL), cytokeratins (ck), bone matrix proteins, enamel matrix proteins (EMPs), inner enamel epithelial (IEE)

Posted Date: March 18th, 2021

DOI: https://doi.org/10.21203/rs.3.rs-295042/v1

License: This work is licensed under a Creative Commons Attribution 4.0 International License.
Read Full License

Version of Record: A version of this preprint was published at Scientific Reports on January 10th, 2022.
See the published version at https://doi.org/10.1038/s41598-021-04091-0.

Analysis of the cells isolated from epithelial cell rests of Malassez through single-cell limiting dilution

Syed Taufiqul Islam[1], Yoshihito Kurashige[1], Dembereldorj Bolortsetseg[1], Erika Minowa[1], Yunosuke Okada[1], Sayaka Sakakibara[1], Yoshihiro Abiko[2] & Masato Saitoh[1*]

[1] Division of Pediatric Dentistry, School of Dentistry, Health Sciences University of Hokkaido, Ishikari Tobetsu, 061-0293, Japan.

[2] Division of Oral Medicine & Pathology, School of Dentistry, Health Sciences University of Hokkaido, Ishikari Tobetsu, 061-0293, Japan.

These authors contributed equally to this work.

Corresponding Author:

Professor Masato Saitoh, D.D.S., Ph.D.

Division of Pediatric Dentistry

School of Dentistry

Health Sciences University of Hokkaido

1757 Kanazawa, Tobetsu, Ishikari, Hokkaido 061-0293, Japan.

E-mail: msaitoh@hoku-iryo-u.ac.jp

Phone: +81-133-23-1211

Abstract

The epithelial cell rests of Malassez (ERM) play a pivotal role in preventing ankylosis between the alveolar bone and the tooth. Although several functions of ERM has been reported, the mechanism behind preventing dentoalveolar ankylosis remains unclear. In this study, 18 clones were isolated from ERM (CRUDE) using the single-cell limiting dilution method. Among them, ERM-2 and -3, which exhibited the highest and lowest proliferation rates, respectively, were selected. ERM-2, ERM-3, and CRUDE ERM were stained with epithelial markers, including cytokeratin-wide and cytokeratin-19, via immunofluorescence. The qRT-PCR analysis revealed increased expression levels of p75 (ameloblast marker), amelogenin, and sfrp5 (inner enamel epithelial cell marker) in the ERM-2 cells. Alternatively, ameloblastin and ck-14 (outer enamel epithelial cell marker) were highly expressed in ERM-3 cells. The mineralization of human periodontal ligament fibroblast (HPDLF) was inhibited when co-cultured with ERM-2, ERM-3, and CRUDE ERM cells. The addition of an anti-amelogenin antibody restored the mineralization of HPDLF cells. Transplanted rat molar cultured in ERM-2 (high amelogenin secretive clone) cell-derived supernatant resulted in significantly smaller bone formation than those cultured in the CRUDE ERM and ERM-3 cell-derived supernatants. These findings indicate that amelogenin produced by ERM cells might be involved in preventing dentoalveolar ankylosis.

Introduction

Periodontal ligament (PDL) is a highly specialized cellular connective tissue that attaches the cementum to the surrounding alveolar bone and holds the tooth within the alveolar socket [1, 2]. In addition, maintenance of the space between the cementum and the alveolar bone is one of the fundamental properties of the PDL. Therefore, the absence of a PDL might lead to early tooth loss and dentoalveolar ankylosis [3]. Epithelial cell rests of Malassez (ERM), the only odontogenic epithelial cells in the PDL tissue, remain quiescent throughout their lifetime. ERM has been shown to maintain the space, homeostasis, and regeneration of PDL [4]. ERM maintains the PDL space by inhibiting cemento-osteogenesis thereby preventing dentoalveolar ankylosis. Conversely, ERM is also thought to be involved in cementum formation during tooth root development [2, 5, 6, 7, 8, 9, 10]. Generally, cells from a subpopulation show harmony in their morphology and function. Alternatively, recent reports have indicated that cells from the same cell line have different morphologies, molecular expression, and functions [11, 12].

Several studies have confirmed the expression of different types of proteins, categorized as cytokeratins (ck), bone matrix proteins, and enamel matrix proteins (EMPs), in ERM [13]. Among them, EMPs are the major secretory proteins of ameloblasts during amelogenesis; they comprise mainly of amelogenin (90%) and non-amelogenin proteins (enamelin, ameloblastin, and amelotin). Among the EMPs, amelogenin is one of the most widely studied proteins in the human body. It plays a significant role in enamel biomineralization during amelogenesis and dictates the width and thickness of the apatite crystals. Amelogenin has been reported to maintain the PDL space [14] and enhance human cementoblast mineralization [15]. The ERM is composed of various cell populations [16], which might account for the different functions of this structure. Although a few cell subtypes in the ERM have been identified in a morphological study [16], the isolation of ERM clones from the different cell populations has not been attempted thus far. We believe that the isolation of single-cell clones from the ERM might aid in

understanding the various functions of this entity. Therefore, the present study aimed to establish clone cells derived from the ERM using the single-cell limiting dilution method. The characteristics of individual ERM clones were determined by evaluating the cell growth rate, secretion of EMPs, and expression levels of the markers of outer enamel epithelial (OEE) and inner enamel epithelial (IEE) cells. The ERM clones were co-cultured with human periodontal ligament fibroblasts (HPDLF) cells to observe the effect of each clone cell on HPDLF cell mineralization. Additionally, the roles of these cells in inducing mineralization and maintaining the PDL spaces were examined in vivo.

Results

Isolated clones from epithelial-like cells exhibited different cell morphologies and proliferation ratios

ERM are the only epithelial-like cells that are present in the PDL space. Therefore, we isolated these cells from the PDL tissue using the outgrowth expansion method (Fig. 1A). A total of 18 clones from the epithelial-like cells were obtained successfully using the single-cell limiting dilution method (Fig. 1B). The clones were named ERM 1–18, and the source material of the clones was named CRUDE ERM. All the clones and the CRUDE ERMs exhibited epithelial-like morphologies in the primary culture. Some of the 18 clones are shown in Figure 1B. Variations in the attachment and growth rate of the cells were observed under a light microscope. The cells were characterized based on their attachment to the surface of the dish and the speed of cell growth (Table 1). The cell attachment was categorized as cobblestone or scattered, and the growth rate was marked as slow, rapid, or average. Working with all 18 clones was difficult, and not all cells had unique phenotypes; hence, clones ERM-2 and -3 along with the CRUDE ERM were selected for further experiments. The growth speeds of the clones were compared with those of the CRUDE ERMs, which were considered as standard or

average. The selection of the cells was performed using the following criteria: CRUDE ERM as the original cell mass from which all clones were obtained; ERM-2, the most rapidly growing cells with a scattered proliferation pattern; and ERM-3, the slowest growing cells with a cobblestone-like proliferation pattern and were most similar to CRUDE ERM.

CyQUANT proliferation assays were performed to further confirm the differences in the proliferation ratios among the three types of cells selected. On day 3, the growth rate of ERM-2 was significantly higher than that of ERM-3. On day 6, the ERM-2 and ERM-3 cells presented with the highest and lowest rates of proliferation, respectively ($p < 0.05$; Fig. 2).

Cell characterization of ERM

Several studies have used ck-wide as a marker for epithelial cells and CK-19 as an ERM marker [17, 18]. In the current study, CRUDE ERM and the clones of ERM-2 and -3 stained positive for both ck-wide and CK-19, confirming their origin as ERM cells. Keratin-positive fibers were observed in the cytoplasm of each cell isolate (Fig. 3).

CRUDE and clone ERMs expressed ameloblast marker p75, amelogenin, and ameloblastin

RT-PCR gel electrophoresis showed that the ERM-2 and -3 clones expressed the highest and lowest levels of p75, respectively (Fig. 4A). In addition, the high p75-expressing cells expressed significantly high levels of amelogenin and low levels of ameloblastin. The cells with the lowest expression level of p75 (ERM-3) expressed significantly lower levels of amelogenin and high levels of ameloblastin (Fig. 4B; $p < 0.05$).

The expression profile of amelogenin production by western blot showed that gingival epithelial (G.E) and ERM-3 produced lower levels of amelogenin compared to the CRUDE

ERM and ERM-2 cells. ERM-2 cells produced the highest amount of amelogenin among all the cell types (Fig. 5)

Expression of OEE and IEE cell markers by real-time RT-PCR

The mRNA expression levels of sfrp5 in the ERM-2 clones were significantly higher than those in the ERM-3 cells ($p < 0.05$; Fig. 4Bc). Alternatively, the mRNA expression levels of ck-14 were significantly higher in ERM-3 cells when compared to those in the ERM-2 cells ($p- < 0.05$; Fig. 4Bd).

Inhibition of HPDLF mineralization in vitro

To identify the EMPs of ERM involved in inhibiting the calcification of HPDLF cells, anti-amelogenin, anti-ameloblastin, and anti-enamelin antibodies were added to the culture system (Fig. 6A), and the relative extent of mineralization was examined by alizarin red staining. On day 30 of the staining, HPDLF cells co-cultured with no cells and G.E showed intense staining, whereas those co-cultured with CRUDE or other clone cells showed no mineralization, although some staining was observed in the ERM-3 cells (Fig. 6Aa). The inhibition of mineralization in HPDLF cells following exposure to CRUDE ERM and clone ERMs was stopped when anti-amelogenin was added to the culture media (Fig. 6Ab). However, recovery was not possible when anti-ameloblastin or anti-enamelin antibodies were added (Fig. 6Ab, c). The results of the quantification of ALP activity were consistent with those of the alizarin red staining (Fig. 6B).

Prevention of dentoalveolar ankylosis in transplanted rat molars regulated by the level of amelogenin secretion from ERM clones

Four weeks after transplantation, the rats were sacrificed to observe the furcation areas in the transplanted teeth via hematoxylin and eosin (H & E) staining (Fig. 7A). Teeth cultured in the control group, fresh keratinocyte basal medium (KBM) and G.E cell-derived supernatants presented with large new alveolar bone formation along with dentoalveolar ankylosis (Fig. 7Aa, b) Large bone formations were observed in the CRUDE ERM and ERM-3 groups (Fig. 7Ac, e), whereas the ERM-2 groups presented with comparatively small bone formations (Fig. 7Ad). No ankylosis between the newly formed alveolar bone and tooth root was observed in any of the experimental groups (Fig. 7Ac, d, e). The number of samples showing ankylosis and bone formation in the furcation area is illustrated in supplementary Table 2. The CRUDE ERM and ERM-2 groups, which presented with the highest secretion of amelogenin in the supernatant, formed significantly smaller bone compared to the KBM and G.E groups, and the ERM-3 groups (which had the lowest secretion of amelogenin in the supernatant), (Fig. 7B). Additionally, CRUDE ERM formed significantly larger bone than ERM-2 (Fig. 7B).

Discussion

To the best of our knowledge, this is the first study to isolate and characterize clones from the ERM using the single-cell limiting dilution method. Eighteen different clones were isolated. Variations in the proliferation of the clones might depend on their maturation status within the ERM. Immature cells proliferate faster than mature or differentiated cells [19]. Therefore, the fastest and slowest proliferative cells (ERM-2 and -3, respectively) were selected for the in vitro and in vivo experiments in the present study. These clones stained positive for both ck-14 and CK-19; hence, the expression of the ameloblast, IEE, and OEE cell markers (p75, sfrp5, and ck14, respectively) was evaluated. p75 is a low-affinity nerve growth factor used as a marker of undifferentiated dental epithelial or ameloblast cells [20, 21]. Sfrp5 is a Wnt signal modulator and has been used as a marker of IEE cells [22]. ck-14 is a member of the keratin

family with a typical intermediate filament of odontogenic epithelium, has been used as a marker of OEE cells [22]. The expression levels of p75 and sfrp5 were high in ERM-2 cells, and that of ck-14 was high in ERM-3 cells. Thus, ERM-2 might be a type of early differentiated ameloblast or IEE cell, whereas ERM-3 might be a type of late differentiated ameloblast or OEE cell. The differentiation of an ameloblast is followed by the secretion of low amounts of amelogenin and high amounts of ameloblastin [21, 23]. ERM-2 expressed high levels of amelogenin and low levels of ameloblastin, whereas ERM-3 expressed low amelogenin and high ameloblastin levels. These expression patterns supported the cell types of ERM-2 and-3 as early and late differentiated ameloblasts, respectively.

ERM cells have been suggested to be involved in the maintenance of the PDL space by inhibiting bone and cementum formation [2, 4, 24]. In the current study, the CRUDE ERM, ERM-2, and ERM-3 cells dramatically inhibited the mineralization of HPDLF cells in the co-culture system. These inhibitory effects were recovered when anti-amelogenin was added to the culture media, but failed when anti-ameloblastin and anti-enamelin were added. Amelogenin might be strongly involved in the inhibitory effects of mineralization. Although the expression level of amelogenin was significantly higher in the ERM-2 than in the ERM-3 or CRUDE ERM cells, no significant inhibitory level was observed among the three cell types. The expression of amelogenin in CRUDE ERM, ERM-2, and ERM-3 cells was detected by Western blot analyses. The production of amelogenin by ERM-3 and CRUDE ERM cells might be sufficient to inhibit mineralization. Faint bands for amelogenin were detected in G.E in the Western blot analysis. G.E was also found to inhibit the mineralization of the HPDLF cells even though the level of inhibition was not as significant as those of the other epithelial cells. The effect of amelogenin on mineralization remains controversial, probably due to the different concentrations of amelogenin. Some in vitro studies showed that amelogenin inhibited and promoted

mineralization at high and low concentrations, respectively [25, 26]. Therefore, the low levels of amelogenin produced by G.E might be sufficient to inhibit the mineralization of HPDLF cells.

The transplantation of rat molars that were cultured in ERM-2 (high amelogenin secretive clone) cell-derived supernatants into the rat abdominal wall resulted in significantly less bone formation compared to those that were cultured in ERM-3 or CRUDE ERM cell-derived supernatants. In the control group, teeth cultured in fresh KBM media or G.E supernatants demonstrated larger bone formation along with dentoalveolar ankylosis. These results indicate that a high concentration of amelogenin might inhibit bone formation in vivo. However, anti-amelogenin did not cause any significant differences in mineralization among the ERM-2, ERM-3, and CRUDE ERM cells in the in vitro co-culture experiments. ERM cells interact with mesenchymal cells in vivo, which could affect the expression levels of some proteins in the ERM cells. The expression levels of EMPs produced by ERM cells were altered in cells co-cultured with mesenchymal cells; amelogenin expression was increased in ERM cells co-cultured with dental pulp cells [27, 28]. Furthermore, the expression levels of KLK4 an enamel matrix proteinase were upregulated in ERM cells co-cultured with fibroblasts [29]. In the current study, the supernatants were collected from cultured CRUDE ERM and ERM clones. Therefore, the in vivo data might not directly reflect the results of the in vitro co-culture experiments in our study. Although there is conflicting data about amelogenin's effect on mineralization in vitro, in vivo studies mainly show that amelogenin induces bone and cementum formation and maintains the PDL spaces [30, 31]. Emdogain consists of 90% amelogenin and aid in cementum formation, periodontal ligament regeneration, and bone formation in intra-bony defects [32, 33, 34]. That implies contradictory data as to inducing bone formation and maintenance of PDL space by regenerating PDL tissues. Pathological bone formation in the PDL space area may cause ankylosis. Hence, physiological bone formation accompanied by remodelling of bone and cementum is needed to maintain the PDL space. Amelogenin has been reported to have

properties other than enamel and bone formation, such as PDL regeneration, cementogenesis and inhibition of osteoclastogenesis [30, 35]. These effects may promote physiological bone formation and inhibit pathological bone formation. Inflammatory reactions and vascularization are vital for the induction of heterotopic bone formation [36]. Emdogain was reported to promote healing with minimal inflammatory response; hence, amelogenin is suspected to possess anti-inflammatory properties [37, 38]. Studies have shown that amelogenin inhibits endothelial cell proliferation and promotes the differentiation of endothelial cells [39, 40]. Therefore, amelogenin might play a role in inhibiting heterotopic bone formation. The bones formed around the roots in the current study represent a type of heterotopic bone formation. Thus, the amelogenin produced by ERM-2 inhibited bone formation and might be involved in preventing dentoalveolar ankylosis. Further investigations are needed to prove this speculation.

In conclusion, as far as we are aware, this study is the first to isolate clone cells from ERM and to demonstrate morphological and functional discrepancies within isolated clones. Based on the experiment herein, we conclude that ERM-secreted amelogenin might be related to the inhibition of heterotopic alveolar bone formation in the PDL space, which may help at preventing dentoalveolar ankylosis. However, further investigations are needed to prove this phenomenon.

Materials and Methods

PDL outgrowth explant

PDL outgrowth explant culture was performed to isolate epithelial-like cells as described previously [41, 42, 43]. Two six-month-old porcine jaws were obtained from the livestock sales division (HOKUREN Federation of Agricultural Co-operatives, Hokkaido, Japan) and transported to our laboratory on ice. Four mandibular first molars were extracted from two six-month-old pigs and washed twice in phosphate-buffered saline solution (PBS). Under a

dissecting microscope, the PDL attached to the middle 2/3rd of the root was separated by a scalpel and transferred to Dulbecco's modified Eagle's medium (DMEM; Sigma-Aldrich) with 10% fetal bovine serum (FBS, Gibco) and 2% penicillin/streptomycin (PEN./STREP., Merck). The dissected PDL tissues were placed at the center of a 6-well culture dish (Trueline) with a minimal amount of fresh DMEM. The explants were initially left undisturbed to increase the likelihood of adherence to the surface of the dish and examined after 5 days. After incubating for 5 days at 37°C in 5% CO_2, 500 µl of culture medium was carefully added to avoid floating the tissues on the culture dish. The medium was changed every 72 h until the PDL cells were sub-confluent; two different layers of cells were visible. A clear demarcating line with epithelial-like cells on the inside and a layer of fibroblast-like cells on the outside was observed adjacent to the PDL tissue (Fig. 1A). The PDL tissue and fibroblast-like cells were scraped out and fresh medium was added, followed by gentle washing with PBS. This was done several times until there were no cells other than the epithelial-like cells. The cells were passaged using 0.25% trypsin 0.1% EDTA solution, and those with passage numbers less than four were used for all experiments in this study.

Single-cell limiting dilution

Epithelial-like cells obtained from PDL tissue were cultured in a 100-mm dish at a concentration of 10^4 cells/ml. The supernatant from the cells was filtered and kept at -30°C to be used for single-cell limiting dilution. Serial dilution was performed by seeding 10 µl of the epithelial-like cells (10^2 cells/ml) in each well of a 96-well plate along with 190 µl of the stored supernatant. After 24 h of incubation, 100 µl of the medium was removed gently by pipetting and replaced with fresh DMEM. Every other day, wells with no colonies or multiple colonies were excluded after checking under a light microscope (CKX 41, Olympus, Tokyo, Japan). Wells with single colonies were trypsinized and passaged into 60-mm dishes after they reached

sub-confluency.

Cell morphology and proliferation assay

Eighteen clones were isolated, initially, and named ERM 1–18. The original cell source from where the clones were obtained was defined as the CRUDE ERM. The isolated ERM clones and CRUDE ERM were passaged into 100-mm dishes at 10^3 cells/ml with DMEM. The cells were monitored closely every day to assess their growth patterns and proliferation ratios. Images were taken using a digital camera for categorization (Fig. 1B; PowerShot A640, Canon, Tokyo, Japan). Three cells were selected for further experiments. The selection criteria for the cells are explained in Table 1. The CyQUANT proliferation assay kit (Thermo Fisher Scientific) was used according to products guideline to re-assess the proliferation ratios of the selected cells, CRUDE ERM, and two ERM clones. The cells (10^4 cells/well) were plated with DMEM in 96-well black-walled clear-bottomed plates (Corning Life Sciences) and incubated at 37°C in 5% CO_2 for 1, 2, 3, and 6 days. On day 6, all samples were thawed at room temperature, and 200 µl of CyQUANT GR dye/cell-lysis buffer was added to each well. The fluorescence activity was measured using a fluorescence microplate reader (Infinite F200, TECAN, Zürich, Switzerland) with filters for 480 nm excitation and 520 nm emission (Fig. 2).

Cell characterization

The cells were grown on a glass chamber slide (Nunc Lab TekR II Chamber slide™, Thermo Fisher Scientific, Waltham, US) and immunolabeling was performed as described previously [44]. Briefly, the cells were incubated with the primary antibodies, rabbit anti-wide spectrum cytokeratin (ck-wide), (1:200, Thermo Fisher) and anti-human cytokeratin-19 (CK-19), (1:200, Dako), and subsequently, the secondary antibodies, Alexa Fluor 488 and 546 Goat anti-rabbit IgG (1:1,000, Thermo Fisher Scientific). The cell nuclei were stained with 1 mg/ml

of DAPI-Fluoromount-G (Southern Biotech) at room temperature for 10 min. After mounting the coverslips, fluorescent images were captured using confocal microscopy (Fig.3, Olympus, Tokyo, Japan).

Qualitative and quantitative reverse transcription-polymerase chain reaction analysis

Total RNA was extracted from the cells via the acid guanidine thiocyanate/phenol-chloroform method, using TRizol. Two micrograms of the RNA sample were reverse-transcribed (SuperScript reverse transcriptase, Invitrogen) according to the manufacturer's instructions using oligo (dT) 12–18 primers (Invitrogen).

For the quantitative real-time reverse transcription-polymerase chain reaction (qRT-PCR), aliquots of total cDNA were amplified with amelogenin, ameloblastin, sfrp5, ck-14, and GAPDH primers using the KAPA SYBR® FAST qPCR Master Mix (KAPA BIOSYSTEMS). GAPDH was used as an internal control. Amplifications were performed using a Light Cycler® Nano (Roche, Basel, Switzerland) using the following program settings: 30 cycles after initial denaturation for 30 s at 94°C, annealing for 30 s at 60°C, and extension for 1 min at 72°C. The relative mRNA expression level of each transcript was normalized against that of GAPDH. The relative quantities of gene-specific mRNAs were calculated using the $2^{-(\Delta\Delta Ct)}$ method [45].

For qualitative RT-PCR, the amplification products for p75 were run on 1.5% agarose gel, and the gel was visualized by ethidium bromide staining. Primer sequences used in this experiment have been provided in supplementary Table 1.

Western blot analysis

Protein was extracted from gingival epithelial (G.E), CRUDE ERM, and the ERM clone cells as described previously [46]. The protein samples (20 µg) were separated by electrophoresis on Mini-PROTEAN TGX™ AnyKD SDS-polyacrylamide gels (BIO-RAD) and transferred to

a nitrocellulose membrane (BIO-RAD). The membrane was incubated overnight with mouse monoclonal anti-amelogenin (1:500; SANTA CRUZ) in Milli-Q water containing 0.2% Tween-20 and 4% skim milk at 4°C. After washing, the membrane was incubated with appropriate horseradish peroxidase-conjugated goat anti-mouse IgGs (Abcam) for 1 h at room temperature. Labeled protein bands were detected using an enhanced chemiluminescence system (LuminoGraph, Tokyo, Japan).

Co-culture

HPDLF cells were kindly provided by Prof. Toshiya Arakawa from the Biochemistry Division, Health Sciences University of Hokkaido, Japan. The calcification assay was performed using HPDLF cells co-cultured with G.E, CRUDE ERM, and clone cells as described previously [5]. The cells (500 µl of 10^5 cells/ml) were grown on collagen III-coated inserts in twelve-well Transwell units along with the CRUDE ERM, ERM-2, and ERM-3 cells (1.5 ml of 10^4 cells/ml); the control group had no cells grown or G.E cells on the bottom. (Cell Culture Insert, Transparent PET Membrane, 12-well 0.4-mm pore size, Corning Life Sciences, New York, US). The calcification-promoting medium (α-MEM, 2% L-glutamine, 1% PEN/STREP, 10% FBS, 10 mM β-glycerophosphate, 25 mg ascorbic acid) was used in the inserts and DMEM (low glucose) was used in the bottom for the G.E, CRUDE ERM, ERM-2, and ERM-3 cells. The mineralization of HPDLF cells was confirmed by Alizarin red staining after 10, 20, and 30 days of culture. Alkaline phosphatase (ALP) activity was quantified in the dissolved Alizarin red stains via spectrophotometrical absorption at a wavelength of 405 nm (Infinite F200, TECAN, Mannedorf, Switzerland). To determine whether amelogenin was involved in the mineralization of the HPDLF cells, antibodies for major EMPs produced by ERM cells (monoclonal anti-amelogenin [1:500], ameloblastin [1:2,000], and enamelin

[1:1,000]; SANTA CRUZ, Texas, US) were added to the culture media of the CRUDE ERM, ERM-2 and -3, and G.E cells.

In vivo transplantation of rat molar

CRUDE ERM, ERM-2 and -3 clones, and G.E cells were cultured on growth factor-free KBM for 4 days. The cell supernatants were filtered and stored at -30°C for organ culture of extracted rat teeth.

The in vivo study was approved by the animal ethics and research committee of the Health Sciences University of Hokkaido (Approval number: 47-2017). All animal experiments were performed according to the Health Sciences University of Hokkaido Committee's strict guidelines on Intramural Animal Use. The handling of the animals in this experiment complied with the ARRIVE guidelines. Twenty 4-week-old male Wistar rats were used for 4 weeks of transplantation. Following anesthesia, the first maxillary molars were extracted and rinsed with DMEM (without serum) to remove blood clots and bone particles. Molars with root fractures were discarded. Three molars were used for each sample. The molars were then transferred into 6-well dishes and cultured with the supernatants of the CRUDE ERM, ERM-2 and -3 clones, and as negative control fresh KBM or G.E cells was used, for 48 h. Subsequently, the teeth were re-transplanted into the abdominal subcutaneous connective tissue of the same animals they were extracted from as previously described [47-49]. At four weeks after transplantation, the transplanted teeth were excised along with portions of the surrounding tissue. They were fixed with 4% paraformaldehyde in 0.1 M phosphate buffer (pH 7.4) at 4°C for 24 h and decalcified in 0.5 mol/L EDTA (pH 7.5) for 20 days at room temperature. The specimens were dehydrated in increasing concentrations of ethanol and embedded in paraffin. Serial sections (thickness, 2 μm) were obtained using a sliding microtome (E. Leitz, Wetzlar, Germany). After deparaffinization with xylene and dehydration with ethanol, some of the

sections were stained with H & E staining (FUJIFILM). The bifurcation area of the roots was observed by light microscopy. Bone formation in each sample was quantified using the images obtained for the light microscopy (same magnification) with the aid of the ImageJ software (https://imagej.nih.gov/ij/).

Statistical analysis

The statistical analyses were conducted using SPSS 26.0 statistical software (IBM, North Castle, NY). Results are expressed as mean ± standard deviation. Comparison among multiple groups was performed using a one-way analysis of variance (ANOVA) and Scheffe's test. A *p*-value <0.05 was considered statistically significant.

References

1 Beertsen, W., McCulloch, C. A. & Sodek, J. The periodontal ligament: a unique, multifunctional connective tissue. *Periodontol 2000* **13**, 20-40, doi:10.1111/j.1600-0757.1997.tb00094.x (1997).

2 Xiong, J., Gronthos, S. & Bartold, P. M. Role of the epithelial cell rests of Malassez in the development, maintenance and regeneration of periodontal ligament tissues. *Periodontol 2000* **63**, 217-233, doi:10.1111/prd.12023 (2013).

3 Pulitano Manisagian, G. E., Benedí, D., Goya, J. A. & Mandalunis, P. M. Study of epithelial rests of Malassez in an experimental periodontitis model. *Acta Odontol Latinoam* **31**, 131-137 (2018).

4 Silva, B. S. E. *et al.* Epithelial rests of Malassez: from latent cells to active participation in orthodontic movement. *Dental Press J Orthod* **22**, 119-125, doi:10.1590/2177-6709.22.3.119-125.sar (2017).

5 Noro, D. *et al.* Effect of epithelial cells derived from periodontal ligament on osteoblast-like cells in a Transwell membrane coculture system. *Arch Oral Biol* **60**, 1007-1012, doi:10.1016/j.archoralbio.2015.02.016 (2015).

6 Lindskog, S., Blomlöf, L. & Hammarström, L. Evidence for a role of odontogenic epithelium in maintaining the periodontal space. *J Clin Periodontol* **15**, 371-373, doi:10.1111/j.1600-051x.1988.tb01014.x (1988).

7 Yamashiro, T., Fujiyama, K., Fukunaga, T., Wang, Y. & Takano-Yamamoto, T. Epithelial rests of Malassez express immunoreactivity of TrkA and its distribution is regulated by sensory nerve innervation. *J Histochem Cytochem* **48**, 979-984, doi:10.1177/002215540004800711 (2000).

8 Brice, G. L., Sampson, W. J. & Sims, M. R. An ultrastructural evaluation of the relationship between epithelial rests of Malassez and orthodontic root resorption and repair in man. *Aust Orthod J* **12**, 90-94 (1991).

9 Suzuki, M. *et al.* Morphology of Malassez's epithelial rest-like cells in the cementum: transmission electron microscopy, immunohistochemical, and TdT-mediated dUTP-biotin nick end labeling studies. *J Periodontal Res* **41**, 280-287, doi:10.1111/j.1600-0765.2006.00871.x (2006).

10 Xiong, J., Mrozik, K., Gronthos, S. & Bartold, P. M. Epithelial cell rests of Malassez contain unique stem cell populations capable of undergoing epithelial-mesenchymal transition. *Stem Cells Dev* **21**, 2012-2025, doi:10.1089/scd.2011.0471 (2012).

11 Hu, P., Zhang, W., Xin, H. & Deng, G. Single Cell Isolation and Analysis. *Front Cell Dev Biol* **4**, 116, doi:10.3389/fcell.2016.00116 (2016).

12
Gross, A. *et al.* Technologies for Single-Cell Isolation. *Int J Mol Sci* **16**, 16897-16919, doi:10.3390/ijms160816897 (2015).
13 Bykov, V. L. [Epithelial cell rests of Malassez: tissue, cell, and molecular biology]. *Morfologiia* **124**, 95-103 (2003).
14 Bansal, A. K., Shetty, D. C., Bindal, R. & Pathak, A. Amelogenin: A novel protein with diverse applications in genetic and molecular profiling. *J Oral Maxillofac Pathol* **16**, 395-399, doi:10.4103/0973-029x.102495 (2012).
15 Tanimoto, K. *et al.* Differential effects of amelogenin on mineralization of cementoblasts and periodontal ligament cells. *J Periodontol* **83**, 672-679, doi:10.1902/jop.2011.110408 (2012).
16 Reeve, C. M. & Wentz, F. M. The prevalence, morphology, and distribution of epithelial rests in the human periodontal ligament. *Oral Surg Oral Med Oral Pathol* **15**, 785-793, doi:10.1016/0030-4220(62)90328-6 (1962).
17 Oka, K. *et al.* Cellular turnover in epithelial rests of Malassez in the periodontal ligament of the mouse molar. *Eur J Oral Sci* **120**, 484-494, doi:10.1111/eos.12003 (2012).
18 Nezu, T., Matsuzaka, K., Nishii, Y., Sueishi, K. & Inoue, T. The effect of aging on the functions of epithelial rest cells of Malassez in vitro: immunofluorescence, DNA microarray and RT-PCR analyses. *Oral Medicine & Pathology* **15**, 101-106, doi:10.3353/omp.15.101 (2011).
19 Cooper, G. M. *The cell : a molecular approach*. (ASM Press ; Sinauer Associates, 2000).
20 Mitsiadis, T. A., Couble, P., Dicou, E., Rudkin, B. B. & Magloire, H. Patterns of nerve growth factor (NGF), proNGF, and p75 NGF receptor expression in the rat incisor: comparison with expression in the molar. *Differentiation* **54**, 161-175, doi:10.1111/j.1432-0436.1993.tb01599.x (1993).
21 Fukumoto, S. *et al.* Ameloblastin is a cell adhesion molecule required for maintaining the differentiation state of ameloblasts. *J Cell Biol* **167**, 973-983, doi:10.1083/jcb.200409077 (2004).
22 Juuri, E. *et al.* Sox2+ stem cells contribute to all epithelial lineages of the tooth via Sfrp5+ progenitors. *Dev Cell* **23**, 317-328, doi:10.1016/j.devcel.2012.05.012 (2012).
23 Kiyosue, T. *et al.* Immunohistochemical location of the p75 neurotrophin receptor (p75NTR) in oral leukoplakia and oral squamous cell carcinoma. *Int J Clin Oncol* **18**, 154-163, doi:10.1007/s10147-011-0358-4 (2013).
24 Lyngstadaas, S. P., Lundberg, E., Ekdahl, H., Andersson, C. & Gestrelius, S. Autocrine growth factors in human periodontal ligament cells cultured on enamel matrix derivative. *J Clin Periodontol* **28**, 181-188, doi:10.1034/j.1600-051x.2001.028002181.x (2001).
25 Viswanathan, H. L. *et al.* Amelogenin: a potential regulator of cementum-associated genes. *J Periodontol* **74**, 1423-1431, doi:10.1902/jop.2003.74.10.1423 (2003).
26 Izumikawa, M., Hayashi, K., Polan, M. A., Tang, J. & Saito, T. Effects of amelogenin on proliferation, differentiation, and mineralization of rat bone marrow mesenchymal stem cells in vitro. *ScientificWorldJournal* **2012**, 879731, doi:10.1100/2012/879731 (2012).

27 Shinmura, Y., Tsuchiya, S., Hata, K. & Honda, M. J. Quiescent epithelial cell rests of Malassez can differentiate into ameloblast-like cells. *J Cell Physiol* **217**, 728-738, doi:10.1002/jcp.21546 (2008).

28 Shiba, H. *et al.* Enhancement of alkaline phosphatase synthesis in pulp cells co-cultured with epithelial cells derived from lower rabbit incisors. *Cell Biol Int* **27**, 815-823, doi:10.1016/s1065-6995(03)00159-8 (2003).

29 Kim, G. H. *et al.* Differentiation and Establishment of Dental Epithelial-Like Stem Cells Derived from Human ESCs and iPSCs. *Int J Mol Sci* **21**, doi:10.3390/ijms21124384 (2020).

30 Haze, A. *et al.* Regeneration of bone and periodontal ligament induced by recombinant amelogenin after periodontitis. *J Cell Mol Med* **13**, 1110-1124, doi:10.1111/j.1582-4934.2009.00700.x (2009).

31 Yagi, Y., Suda, N., Yamakoshi, Y., Baba, O. & Moriyama, K. In vivo application of amelogenin suppresses root resorption. *J Dent Res* **88**, 176-181, doi:10.1177/0022034508329451 (2009).

32 Shirakata, Y. *et al.* Healing of two-wall intra-bony defects treated with a novel EMD-liquid-A pre-clinical study in monkeys. *J Clin Periodontol* **44**, 1264-1273, doi:10.1111/jcpe.12825 (2017).

33 Sculean, A. *et al.* Ten-year results following treatment of intra-bony defects with enamel matrix proteins and guided tissue regeneration. *J Clin Periodontol* **35**, 817-824, doi:10.1111/j.1600-051X.2008.01295.x (2008).

34 Gestrelius, S., Lyngstadaas, S. P. & Hammarström, L. Emdogain--periodontal regeneration based on biomimicry. *Clin Oral Investig* **4**, 120-125, doi:10.1007/s007840050127 (2000).

35 Deutsch, D. *et al.* Amelogenin, a major structural protein in mineralizing enamel, is also expressed in soft tissues: brain and cells of the hematopoietic system. *Eur J Oral Sci* **114 Suppl 1**, 183-189; discussion 201-182, 381, doi:10.1111/j.1600-0722.2006.00301.x (2006).

36 Łęgosz, P., Drela, K., Pulik, Ł., Sarzyńska, S. & Małdyk, P. Challenges of heterotopic ossification-Molecular background and current treatment strategies. *Clin Exp Pharmacol Physiol* **45**, 1229-1235, doi:10.1111/1440-1681.13025 (2018).

37 Myhre, A. E. *et al.* Anti-inflammatory properties of enamel matrix derivative in human blood. *J Periodontal Res* **41**, 208-213, doi:10.1111/j.1600-0765.2005.00863.x (2006).

38 Yotsumoto, K. *et al.* Amelogenin Downregulates Interferon Gamma-Induced Major Histocompatibility Complex Class II Expression Through Suppression of Euchromatin Formation in the Class II Transactivator Promoter IV Region in Macrophages. *Front Immunol* **11**, 709, doi:10.3389/fimmu.2020.00709 (2020).

39 Jonke, E. *et al.* Effect of tyrosine-rich amelogenin peptide on behavior and differentiation of endothelial cells. *Clin Oral Investig* **20**, 2275-2284, doi:10.1007/s00784-016-1726-2 (2016).

40 Almqvist, S., Kleinman, H. K., Werthén, M., Thomsen, P. & Agren, M. S. Effects of amelogenins on angiogenesis-associated processes of endothelial cells. *J Wound Care* **20**, 68, 70-65, doi:10.12968/jowc.2011.20.2.68 (2011).

41 Tanaka, K. *et al.* Comparison of characteristics of periodontal ligament cells obtained from outgrowth and enzyme-digested culture methods. *Arch Oral Biol* **56**, 380-388, doi:10.1016/j.archoralbio.2010.10.013 (2011).

42 Kurashige, Y. *et al.* Profiling of differentially expressed genes in porcine epithelial cells derived from periodontal ligament and gingiva by DNA microarray. *Arch Oral Biol* **53**, 437-442, doi:10.1016/j.archoralbio.2007.12.005 (2008).

43 Yoshida, K. *et al.* Direct reprogramming of epithelial cell rests of malassez into mesenchymal-like cells by epigenetic agents. *Sci Rep* **11**, 1852, doi:10.1038/s41598-020-79426-4 (2021).

44 Lee, J. H. *et al.* Upregulation of GM-CSF by TGF-β 1 in epithelial mesenchymal transition of human HERS/ERM cells. *In Vitro Cell Dev Biol Anim* **50**, 399-405, doi:10.1007/s11626-013-9712-3 (2014).

45 Livak, K. J. & Schmittgen, T. D. Analysis of relative gene expression data using real-time quantitative PCR and the 2(-Delta Delta C(T)) Method. *Methods* **25**, 402-408, doi:10.1006/meth.2001.1262 (2001).

46 Islam, S. *et al.* DNA hypermethylation of sirtuin 1 (SIRT1) caused by betel quid chewing-a possible predictive biomarker for malignant transformation. *Clin Epigenetics* **12**, 12, doi:10.1186/s13148-019-0806-y (2020).

47 Hosoya, A. *et al.* Alveolar bone regeneration of subcutaneously transplanted rat molar. *Bone* **42**, 350-357, doi:10.1016/j.bone.2007.09.054 (2008).

48 Hasan, M. R. *et al.* Effects of tooth storage media on periodontal ligament preservation. *Dent Traumatol* **33**, 383-392, doi:10.1111/edt.12351 (2017).

49 Hamamoto, Y., Hamamoto, N., Nakajima, T. & Ozawa, H. Morphological changes of epithelial rests of Malassez in rat molars induced by local administration of N-methylnitrosourea. *Arch Oral Biol* **43**, 899-906, doi:10.1016/s0003-9969(98)00021-1 (1998).

Authors contribution

S. TI, Y.K and M.S have designed the study. S. TI, Y.K, D.B, E.M, Y.O, and S.S have been involved in data collection and analysis from in vitro. S. TI and Y.K have collected and analyzed the in vivo data. S. TI, Y.K, Y.A and M.S have been involved in data interpretation. S. TI, Y.K, Y.A and M.S have been involved in drafting the manuscript and revising it critically and have given final approval of the version to be published.

Competing Interest

The authors declare no competing interests.

Figure Legends

Figure 1. Epithelial-like cell outgrowth from the periodontal ligament (PDL) tissue explant and isolated clones from epithelial-like cells. **A.** The image shows a PDL outgrowth explant with cells growing out from the tissue at day 15; **a**. PDL tissue, **b.** epithelial-like cells, **c.** fibroblast-like cells. PDL tissue and fibroblast-like cells were scraped followed by washing with PBS. The epithelial-like cells were allowed to grow until confluency (magnification, 60×). **B.** Eighteen clones were isolated from the epithelial-like cells collected from the PDL tissue. Some of the clones are shown here and categorized based on the speed (average, slow, and rapid) and pattern (cobblestone and scattered) of growth of the cells (magnification, 16×).

Figure 2: Proliferation assay of the CRUDE ERM, ERM-2, and ERM-3 cells using a CyQUANT proliferation kit. The cells were plated (10^4 cells/well) and cultured for days 1, -2, -3, and –6. On day 3, ERM-2 showed a significantly high proliferation ratio compared to ERM-3. On day 6, ERM-2 and ERM-3 cells had higher and lower proliferation ratios, respectively. *$p < 0.05$), n = 3.

Figure 3. Immunofluorescence staining of cytokeratin-wide (ck-wide) and cytokeratin-19 (CK-19) in the CRUDE ERM and clone ERMs. All three cell types stained positive for both markers in the cytoplasm. Blue color indicates DAPI and green reflects CK-wide. Scale bar = x, y: 20 µm.

Figure 4. mRNA expression analysis of p75, amelogenin, ameloblastin, sfrp5, and ck-14 using RT-PCR and qRT-PCR. **A.** All the cells expressed for p75. ERM-2 and ERM-3 cells expressed high and low levels of the marker, respectively. **B.** Bar graphs comparing the levels of the

markers among the cell types. **a.** ERM-2 and ERM-3 showed significantly high and low levels of amelogenin expression, respectively, when compared to the other cells. **b.** The expression level of ameloblastin in the ERM-3 cells was significantly higher than those in the other cells, **c.** The expression level of sfrp5 was significantly higher in the ERM-2 cells compared to the CRUDE ERM and ERM-3. **d.** ERM-3 showed a significantly higher level of ck-14 when compared to the CRUDE ERM and ERM-2 cells.

Figure 5. The levels of amelogenin protein production in the gingival epithelial (G.E), CRUDE ERM, and ERM-2 and -3 clone cells analyzed by Western blotting (cropped image; full-length blots are presented in Supplementary Figure 1). ERM-2 cells presented with the highest expression levels of amelogenin protein when compared to the other cells. G.E cells were used as negative control and expressed the least amount of the marker among the various cell types examined.

Figure 6. Alizarin red staining of human periodontal ligament fibroblast (HPDLF) cells co-cultured with G.E, CRUDE ERM, ERM-2, and ERM-3 cells followed by quantification of ALP activity. **A.** Mineralization was examined by Alizarin red staining of the co-culture dishes on day 30. **a.** The HPDLF cells alone and those with G.E showed intense staining of Alizarin red when compared to the HPDLF + CRUDE and HPDLF + ERM clone cells. Mild staining was observed in the HPDLF + ERM-3 cells **b.** The inhibition of HPDLF mineralization was recovered in all groups when anti-amelogenin antibody was added, as seen by the staining with Alizarin red in the cells. **c, d.** The addition of anti-ameloblastin and anti-enamelin did not affect the inhibitory actions of the CRUDE ERM and clones cells on the HPDLF cells (magnification, 16×). The red areas represent alkaline phosphatase staining. **B.** Bar graphs comparing the ALP activities among the cell types. **a.** The CRUDE ERM and clone ERM cells showed significantly

less mineralization activity when compared to the HPDLF alone and HPDLF + G.E cells. **b.** Following the addition of the anti-amelogenin antibody, the ALP activities were recovered in the CRUDE ERM and clone cells. **c, d.** The addition of anti-ameloblastin and anti-enamelin resulted in significantly less mineralization in the CRUDE ERM and clone ERM cells when compared to the HPDLF alone and HPDLF + G.E cells. * $p < 0.05$.

Figure 7. Hematoxylin-eosin (H &E) staining and measurement of newly formed bones in rat mandibular first molar furcation area. **A.** Micrographs of the bifurcation areas of the roots. **a,b.** The teeth cultured in control group (fresh KBM and G.E supernatant) demonstrated larger areas of bone formation along with dentoalveolar ankylosis. **c, d, e** Teeth cultured in supernatants from the CRUDE ERM and ERM-2 cells formed smaller areas of new bone compare to those cultured in ERM-3 cell-derived supernatant; none of the experimental groups developed dentoalveolar ankylosis. Scale bar = 100 μm. **B.** Bar graph comparing the quantity of bone formation among the various groups (n = 3). The teeth cultured in supernatants derived from the CRUDE ERM and ERM-2 cells (cells with highest levels of amelogenin) demonstrated significantly lower areas of bone formation compared to those cultured in the supernatants derived from ERM-3 cells (lowest level of amelogenin), G.E cells, and KBM. Additionally, teeth cultured in CRUDE ERM cell-derived supernatant demonstrated significantly larger bone formations than those cultured in ERM-2 cell-derived supernatant.

Table 1. Comparison of CRUDE ERM and clones ERM 1-18 based on visual observations and digital images.

Table 1

Cell name	Growth speed	Growth pattern
CRUDE	**considered as standard/average**	**cobblestone**
ERM-1	**average**	**scattered**
ERM-2	**rapid**	**scattered**
ERM-3	**slow**	**cobblestone**
ERM-4	**average**	**cobblestone**
ERM-5	**average**	**scattered**
ERM-6	**slow**	**cobblestone**
ERM-7	**average**	**cobblestone**
ERM-8	**average**	**cobblestone**
ERM-9	**rapid**	**cobblestone**
ERM-10	**average**	**scattered**
ERM-11	**rapid**	**cobblestone**
ERM-12	**rapid**	**cobblestone**
ERM-13	**average**	**cobblestone**
ERM-14	**average**	**cobblestone**
ERM-15	**average**	**scattered**
ERM-16	**average**	**scattered**
ERM-17	**average**	**cobblestone**
ERM-18	**slow**	**scattered**

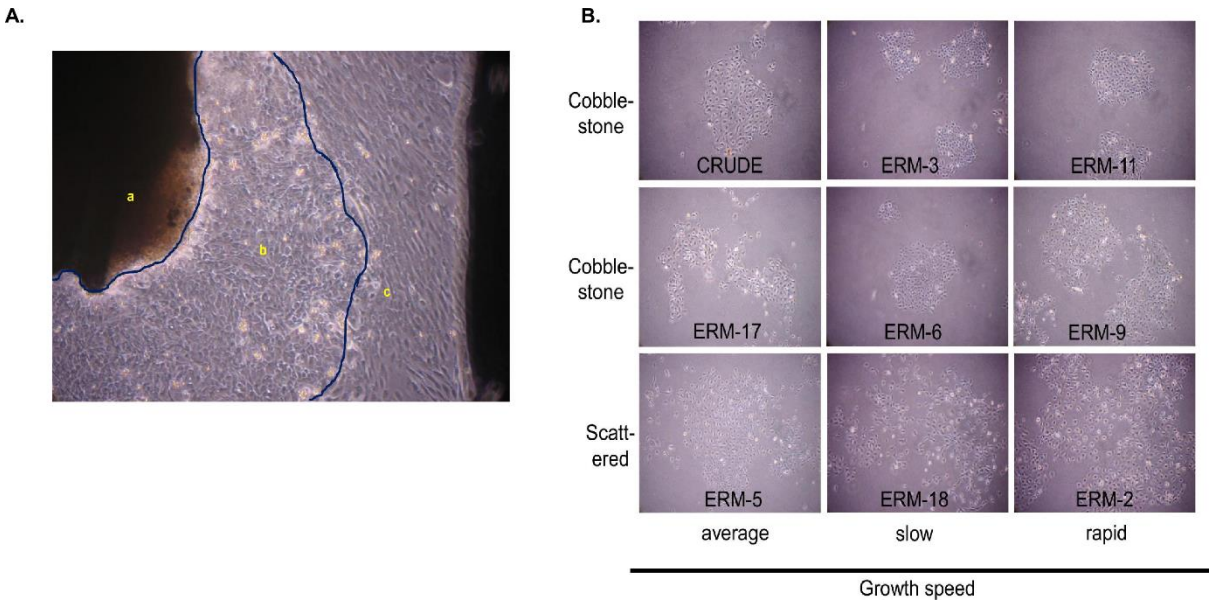
A.
a
b
c
B.
Cobble-stone
Cobble-stone
Scatt-ered
CRUDE
ERM-3
ERM-11
ERM-17
ERM-6
ERM-9
ERM-5
ERM-18
ERM-2
average
slow
rapid
Growth speed

Fig. 1 A.B

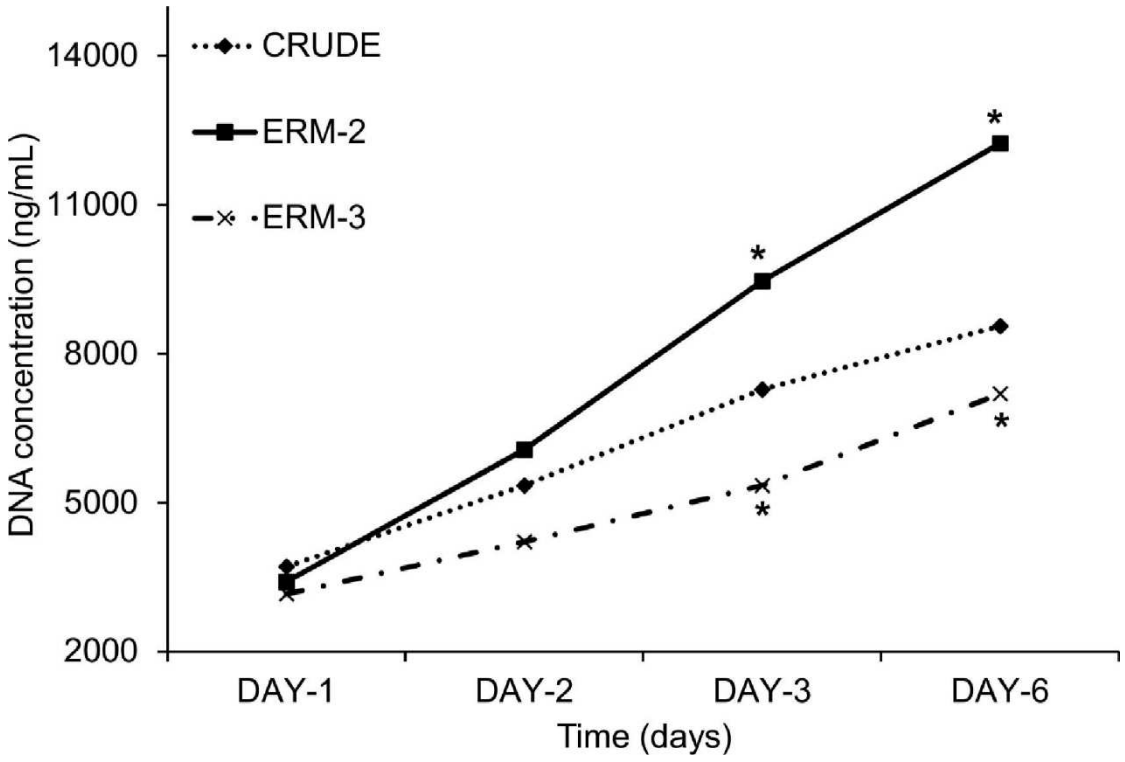
CRUDE
ERM-2
ERM-3
14000
11000
8000
5000
2000
DNA concentration (ng/mL)
DAY-1
DAY-2
DAY-3
DAY-6
Time (days)
*
*
*
*

Fig. 2

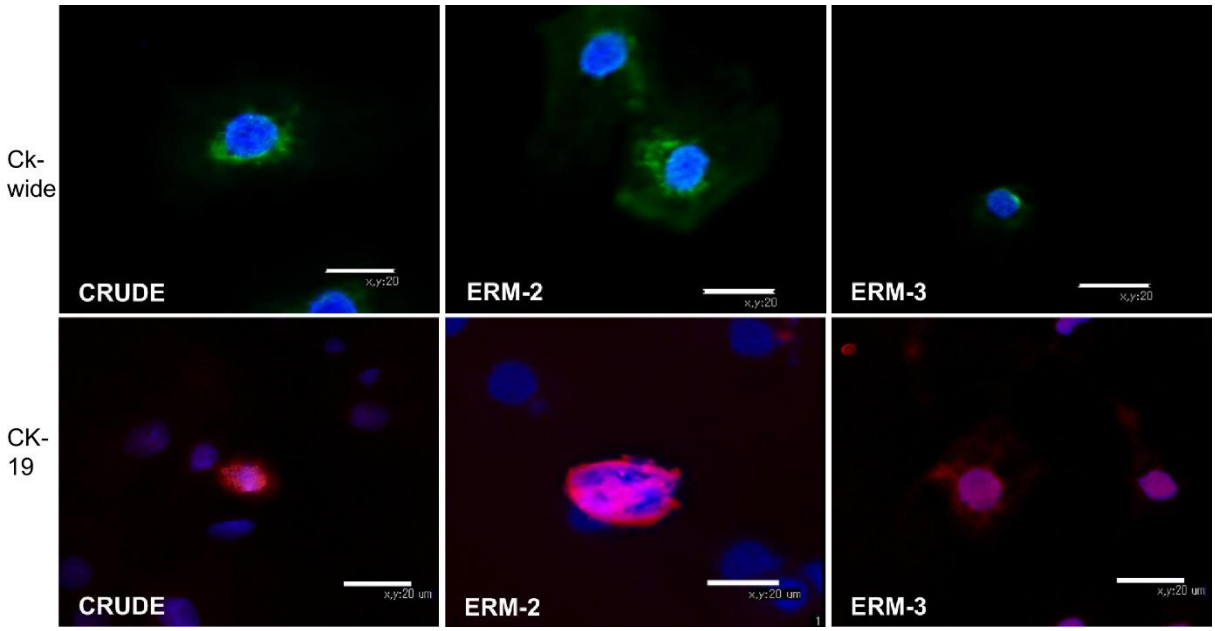
Ck-
wide
CRUDE
x,y:20
ERM-2
x,y:20
ERM-3
x,y:20
CK-
19
CRUDE
x,y:20 um
ERM-2
x,y:20 um
ERM-3
x,y:20 um

Fig. 3

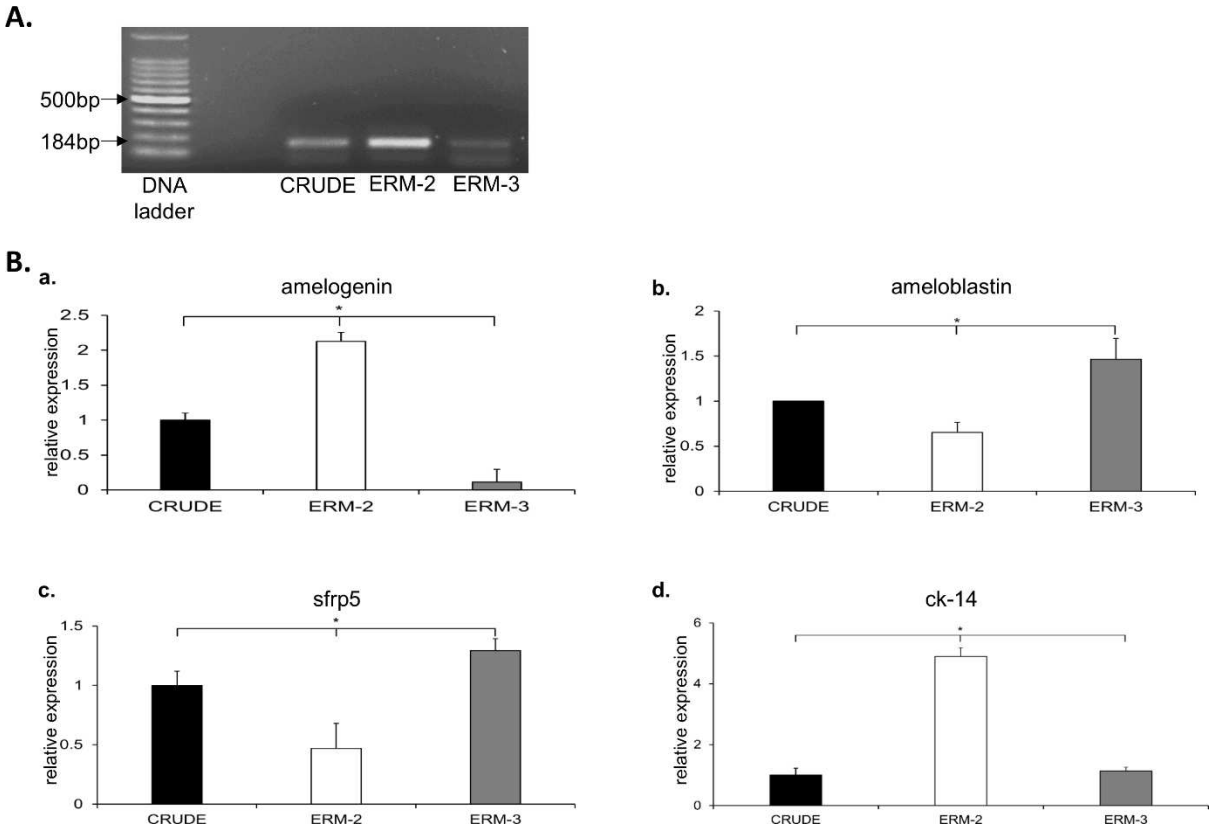
A.
500bp
184bp
DNA ladder
CRUDE
ERM-2
ERM-3
B.
a.
amelogenin
relative expression
2.5
2
1.5
1
0.5
0
CRUDE
ERM-2
ERM-3
b.
ameloblastin
relative expression
2
1.5
1
0.5
0
CRUDE
ERM-2
ERM-3
c.
sfrp5
relative expression
1.5
1
0.5
0
CRUDE
ERM-2
ERM-3
d.
ck-14
relative expression
6
4
2
0
CRUDE
ERM-2
ERM-3

Fig. 4 A, B

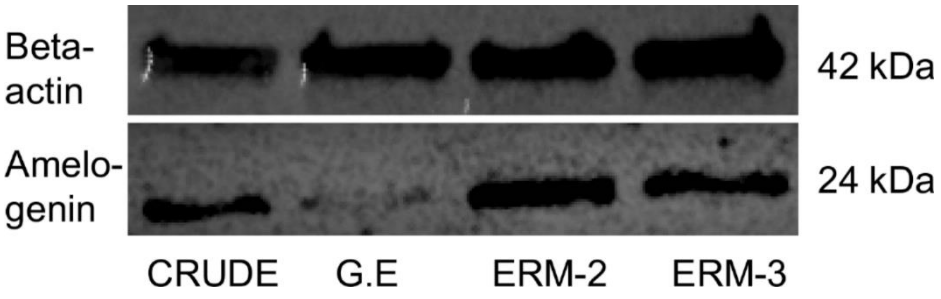

Fig. 5

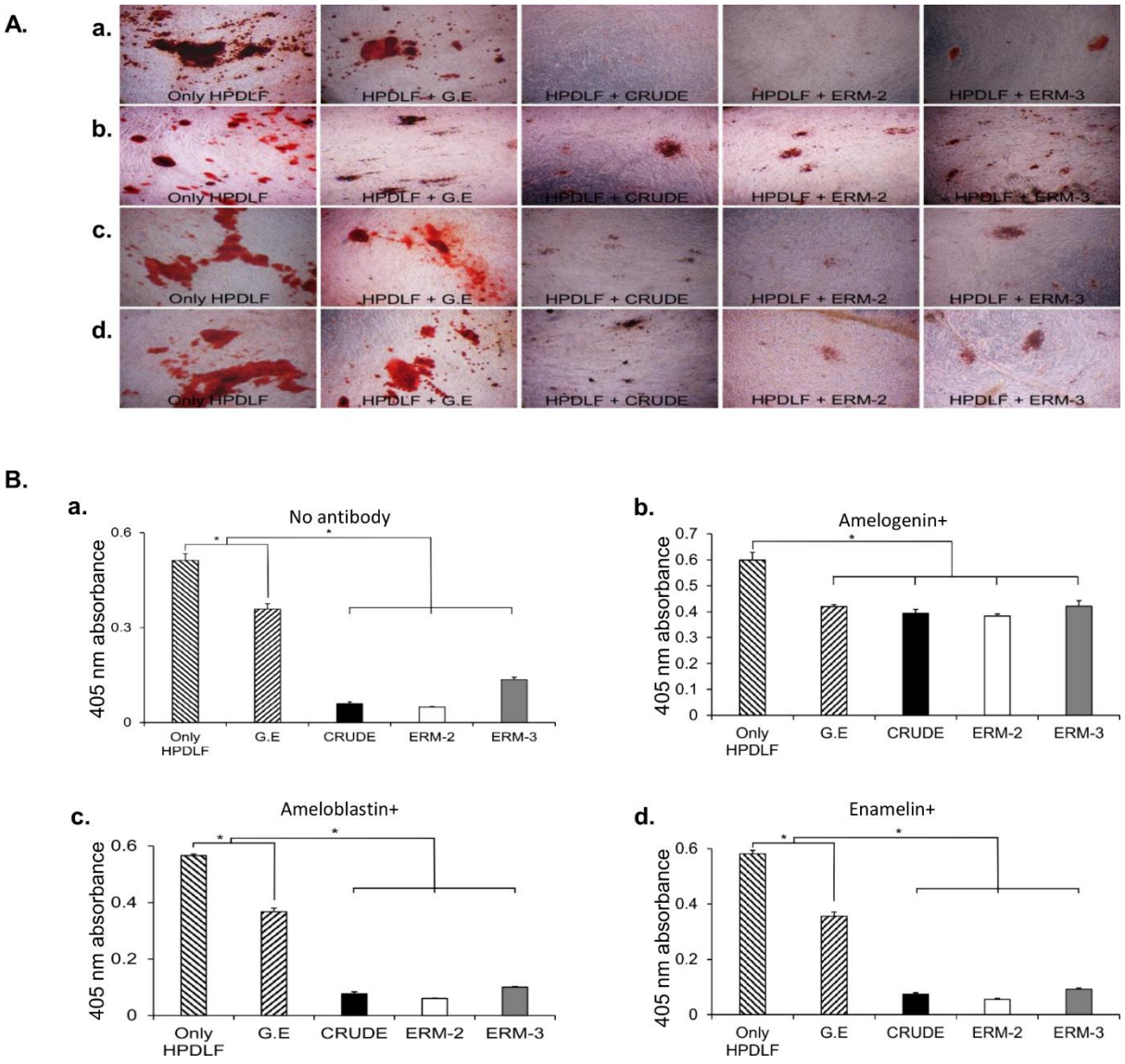
A.
a.
b.
c.
d.
Only HPDLF
HPDLF + G.E
HPDLF + CRUDE
HPDLF + ERM-2
HPDLF + ERM-3
B.
a.
No antibody
b.
Amelogenin+
c.
Ameloblastin+
d.
Enamelin+
405 nm absorbance
Only HPDLF
G.E
CRUDE
ERM-2
ERM-3

Fig. 6 A. B

A.

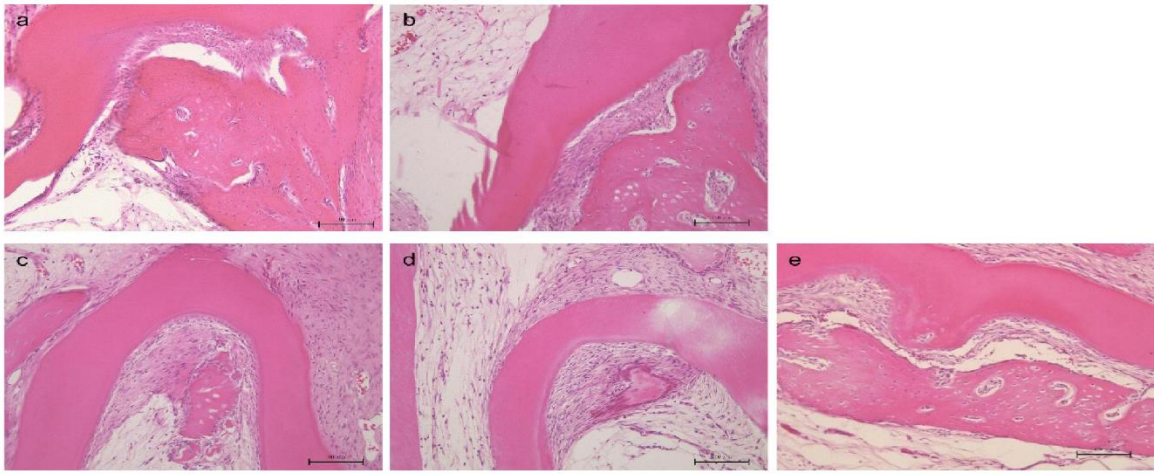
a
b
c
d
e

B.

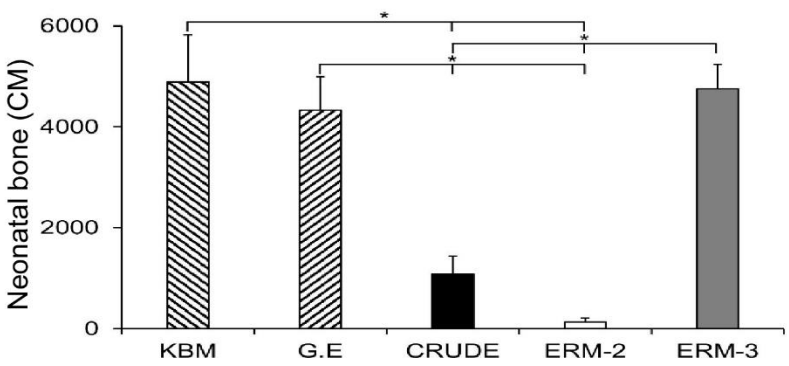
Neonatal bone (CM)
6000
4000
2000
0
KBM
G.E
CRUDE
ERM-2
ERM-3
*
*
*

Fig. 7 A. B

Figures

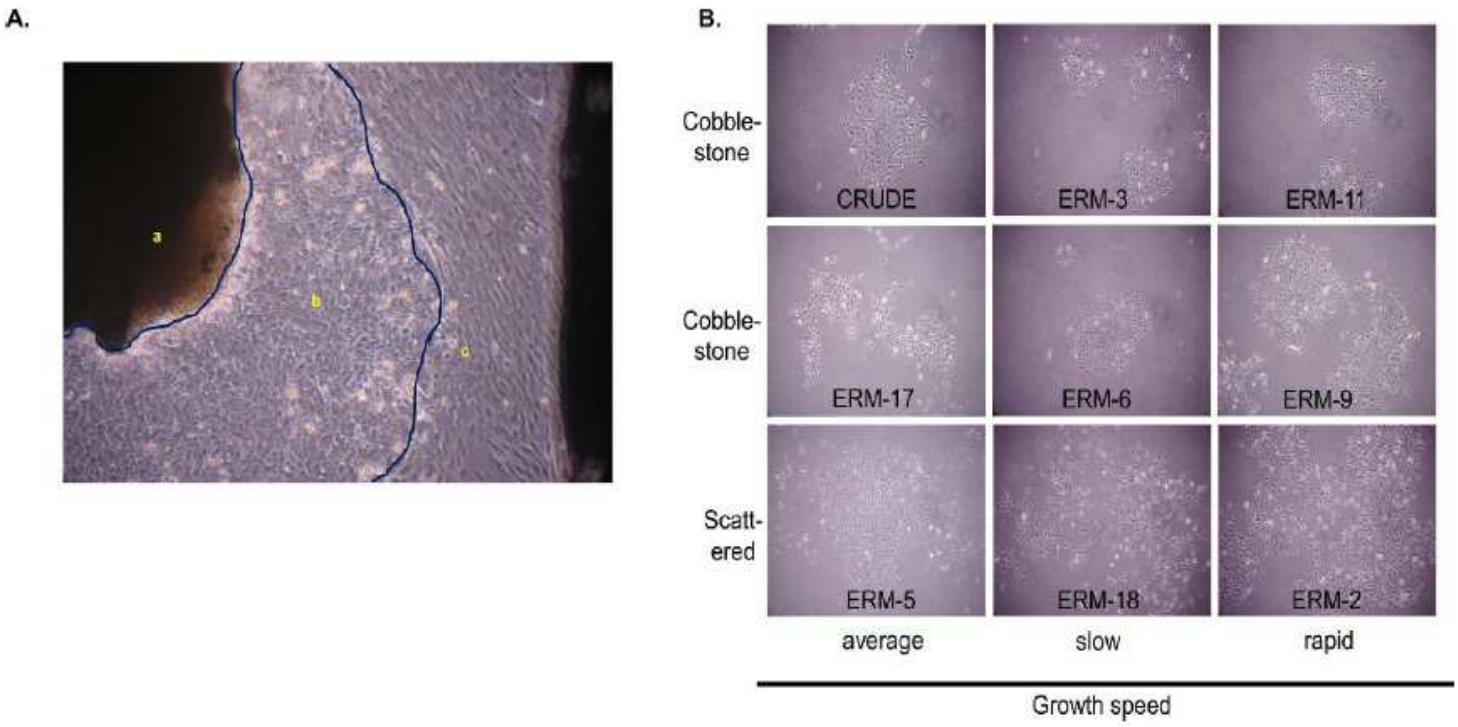

Figure 1

Epithelial-like cell outgrowth from the periodontal ligament (PDL) tissue explant and isolated clones from epithelial-like cells. A. The image shows a PDL outgrowth explant with cells growing out from the tissue at day 15; a. PDL tissue, b. epithelial-like cells, c. fibroblast-like cells. PDL tissue and fibroblast-like cells were scraped followed by washing with PBS. The epithelial-like cells were allowed to grow until confluency (magnification, 60×). B. Eighteen clones were isolated from the epithelial-like cells collected from the PDL tissue. Some of the clones are shown here and categorized based on the speed (average, slow, and rapid) and pattern (cobblestone and scattered) of growth of the cells (magnification, 16×).

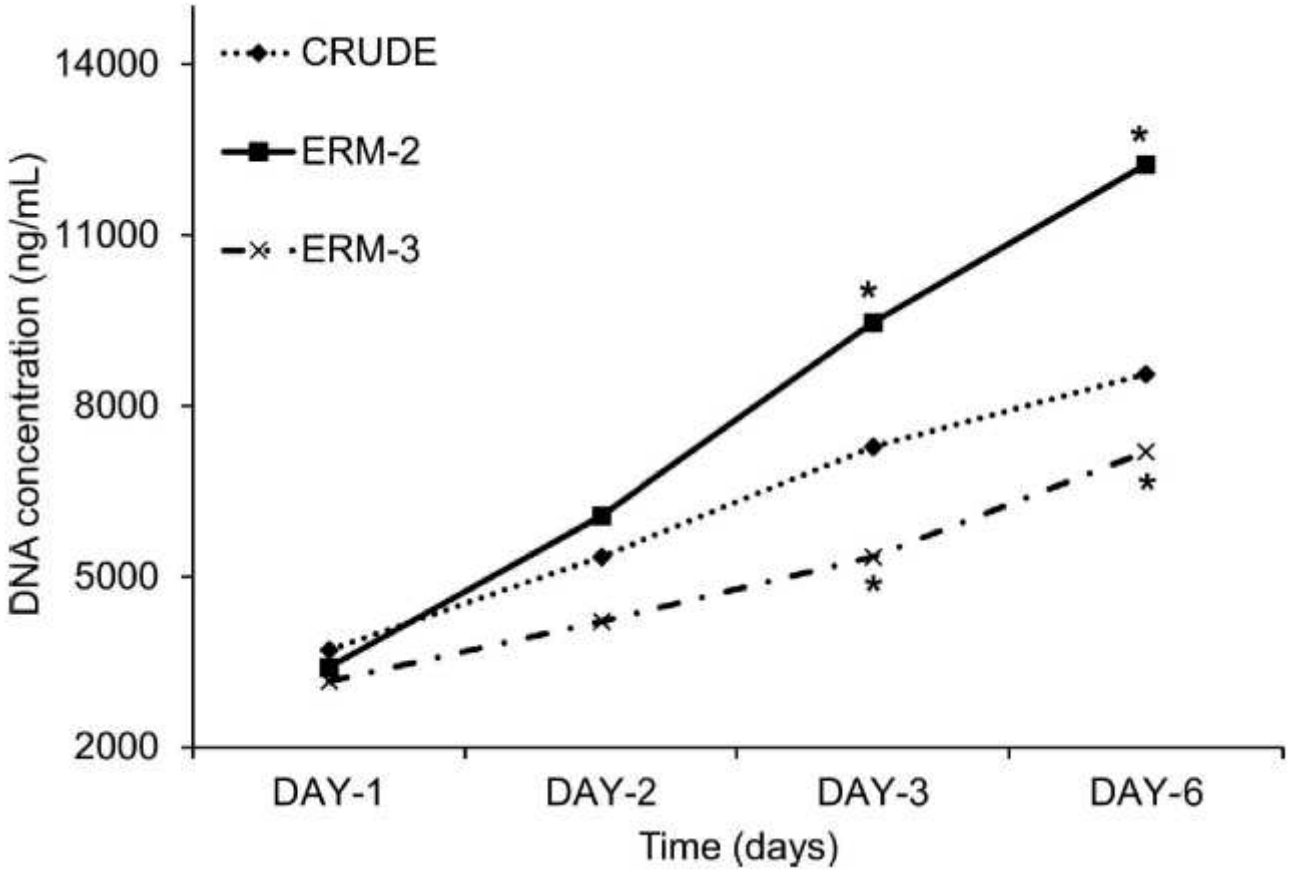

Figure 2

Proliferation assay of the CRUDE ERM, ERM-2, and ERM-3 cells using a CyQUANT proliferation kit. The cells were plated (104 cells/well) and cultured for days 1, -2, -3, and –6. On day 3, ERM-2 showed a significantly high proliferation ratio compared to ERM-3. On day 6, ERM-2 and ERM-3 cells had higher and lower proliferation ratios, respectively. *$p < 0.05$), $n = 3$.

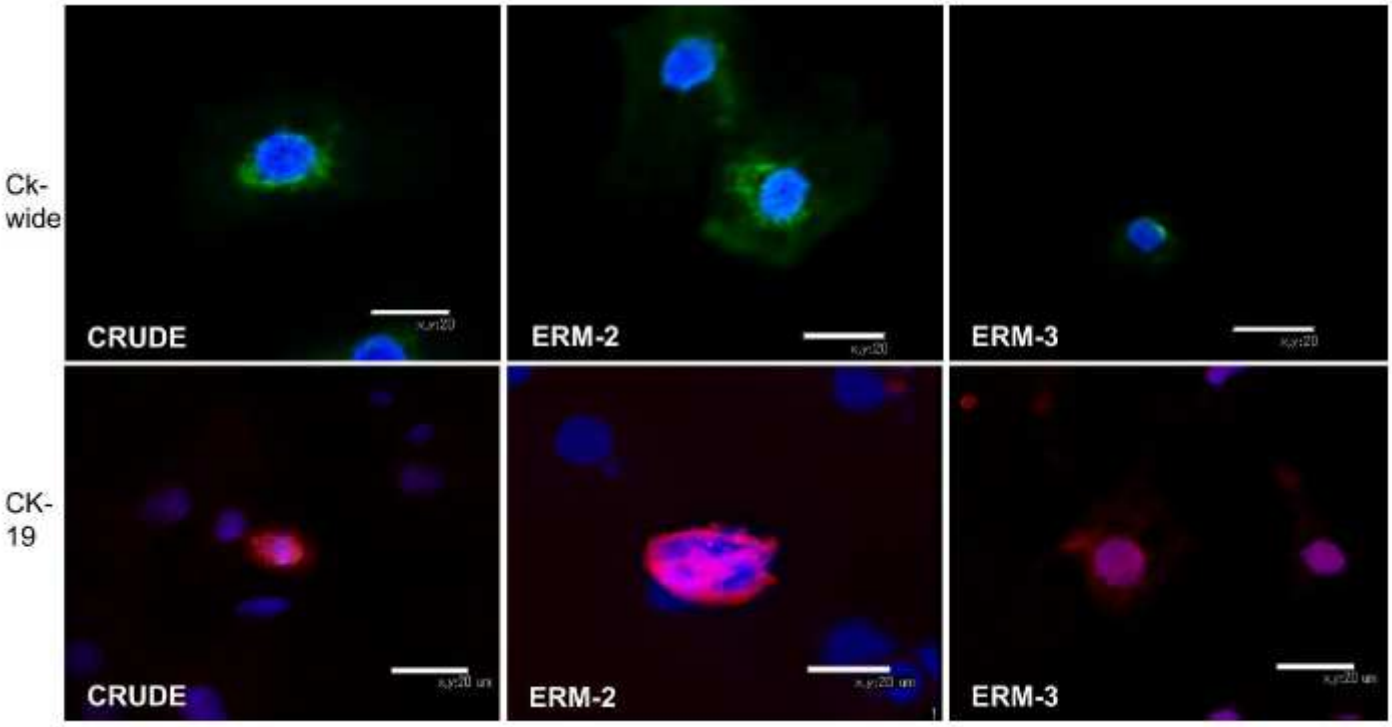

Figure 3

Immunofluorescence staining of cytokeratin-wide (ck-wide) and cytokeratin-19 (CK-19) in the CRUDE ERM and clone ERMs. All three cell types stained positive for both markers in the cytoplasm. Blue color indicates DAPI and green reflects CK-wide. Scale bar = x, y: 20 µm.

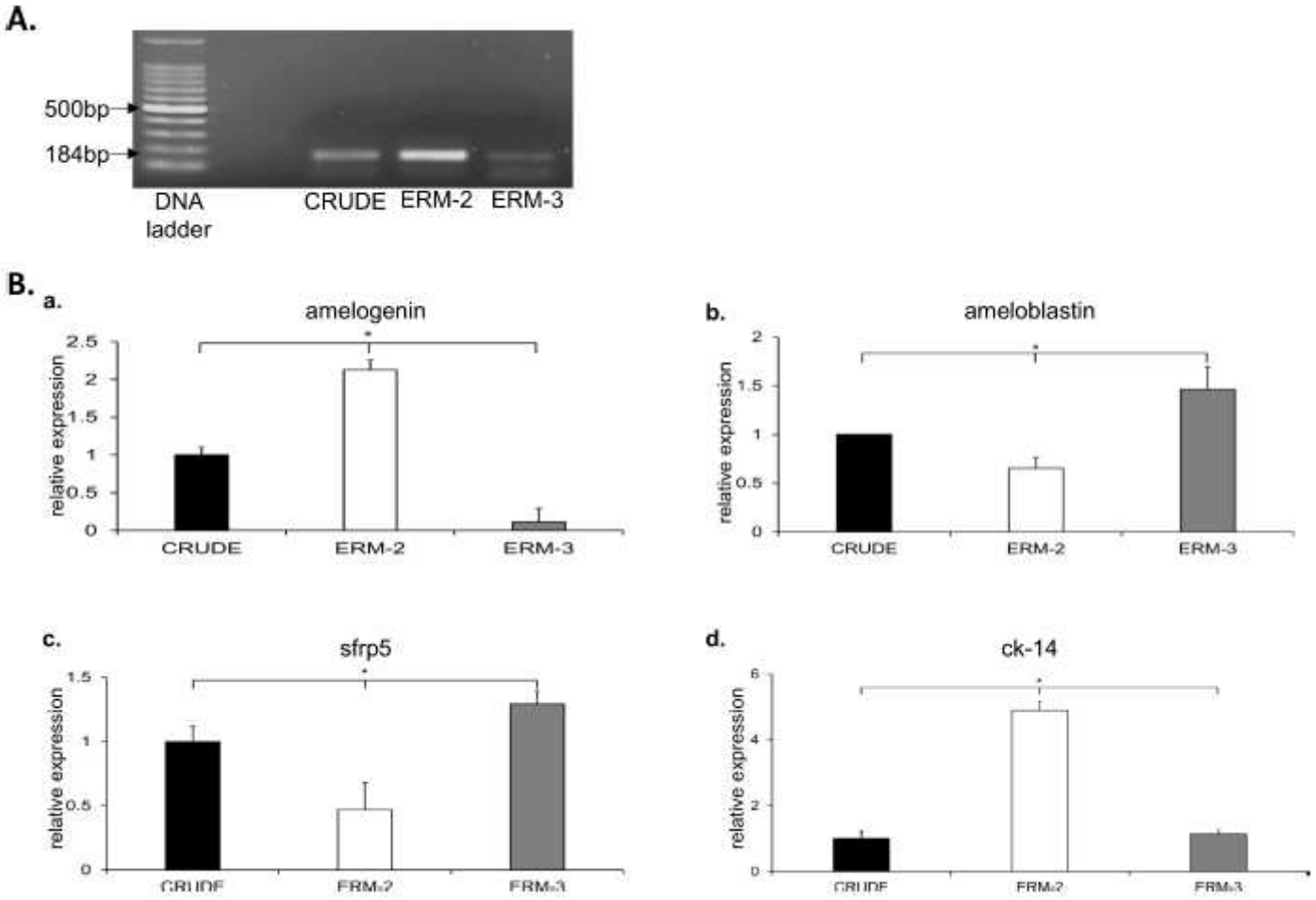

Figure 4

mRNA expression analysis of p75, amelogenin, ameloblastin, sfrp5, and ck-14 using RT-PCR and qRT-PCR. A. All the cells expressed for p75. ERM-2 and ERM-3 cells expressed high and low levels of the marker, respectively. B. Bar graphs comparing the levels of the markers among the cell types. a. ERM-2 and ERM-3 showed significantly high and low levels of amelogenin expression, respectively, when compared to the other cells. b. The expression level of ameloblastin in the ERM-3 cells was significantly higher than those in the other cells, c. The expression level of sfrp5 was significantly higher in the ERM-2 cells compared to the CRUDE ERM and ERM-3. d. ERM-3 showed a significantly higher level of ck-14 when compared to the CRUDE ERM and ERM-2 cells.

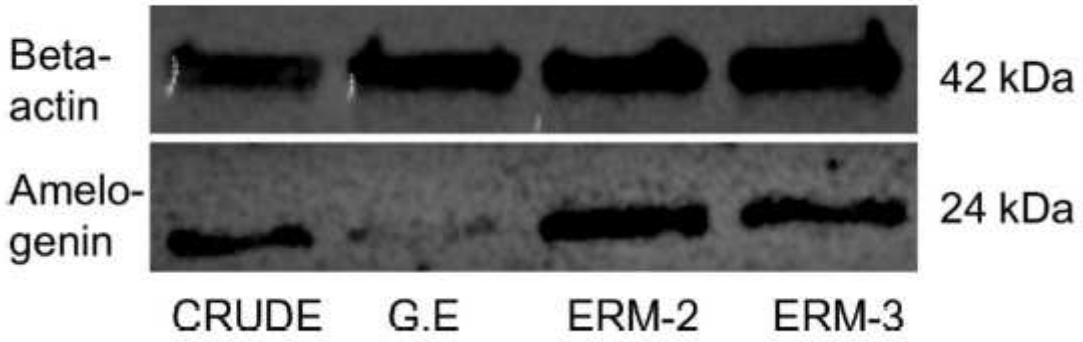

Figure 5

The levels of amelogenin protein production in the gingival epithelial (G.E), CRUDE ERM, and ERM-2 and -3 clone cells analyzed by Western blotting (cropped image; full-length blots are presented in Supplementary Figure 1). ERM-2 cells presented with the highest expression levels of amelogenin protein when compared to the other cells. G.E cells were used as negative control and expressed the least amount of the marker among the various cell types examined.

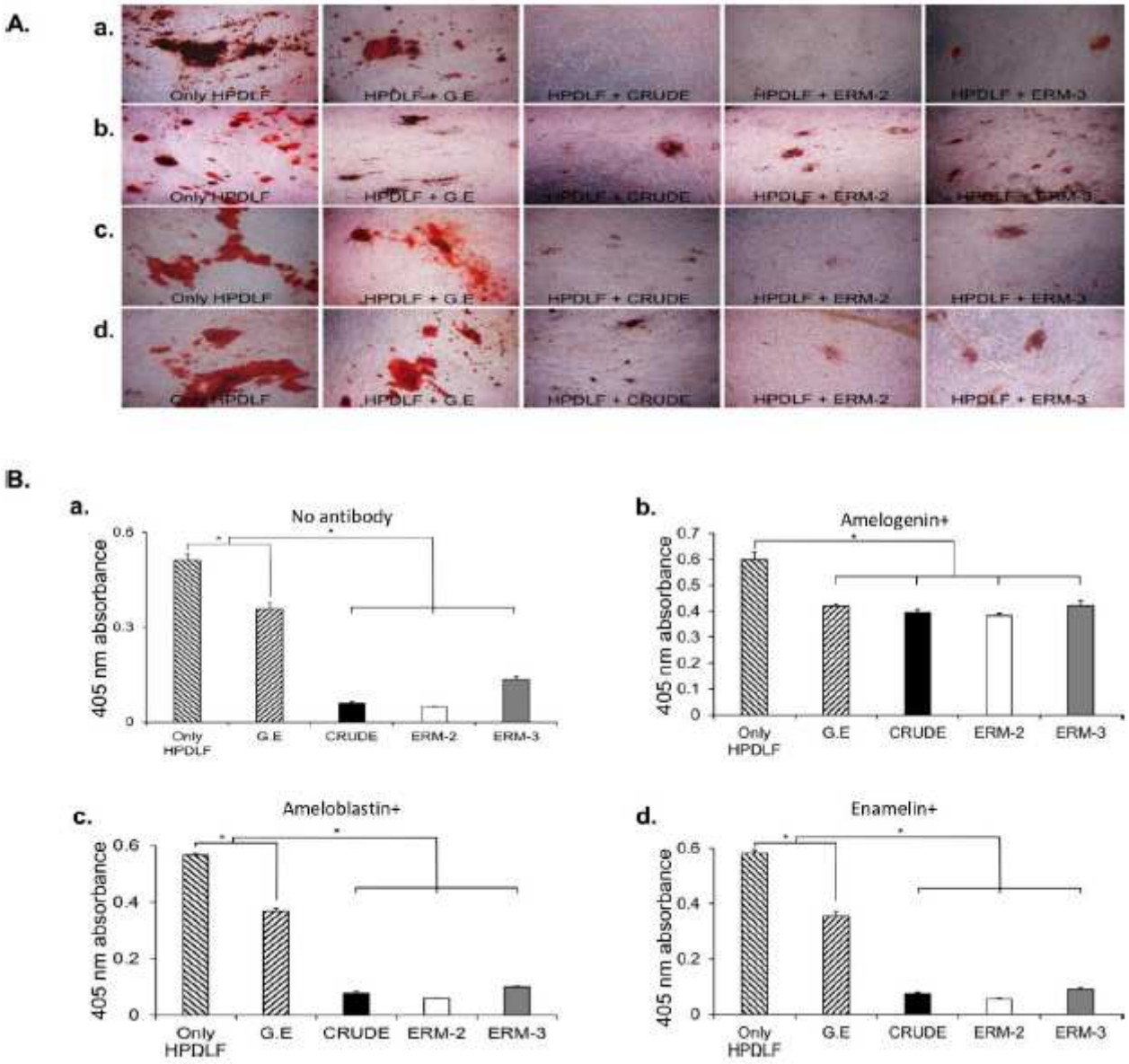

Figure 6

Alizarin red staining of human periodontal ligament fibroblast (HPDLF) cells co-cultured with G.E, CRUDE ERM, ERM-2, and ERM-3 cells followed by quantification of ALP activity. A. Mineralization was examined by Alizarin red staining of the co-culture dishes on day 30. a. The HPDLF cells alone and those with G.E showed intense staining of Alizarin red when compared to the HPDLF + CRUDE and HPDLF + ERM clone cells. Mild staining was observed in the HPDLF + ERM-3 cells b. The inhibition of HPDLF mineralization was recovered in all groups when anti-amelogenin antibody was added, as seen by the staining with Alizarin red in the cells. c, d. The addition of anti-ameloblastin and anti-enamelin did not affect the inhibitory actions of the CRUDE ERM and clones cells on the HPDLF cells (magnification, 16×). The red areas represent alkaline phosphatase staining. B. Bar graphs comparing the ALP activities among the cell types. a. The CRUDE ERM and clone ERM cells showed significantly less mineralization activity when compared to the HPDLF alone and HPDLF + G.E cells. b. Following the addition of the anti-amelogenin antibody, the ALP activities were recovered in the CRUDE ERM and clone cells. c, d. The addition of anti-

ameloblastin and anti-enamelin resulted in significantly less mineralization in the CRUDE ERM and clone ERM cells when compared to the HPDLF alone and HPDLF + G.E cells. * $p < 0.05$.

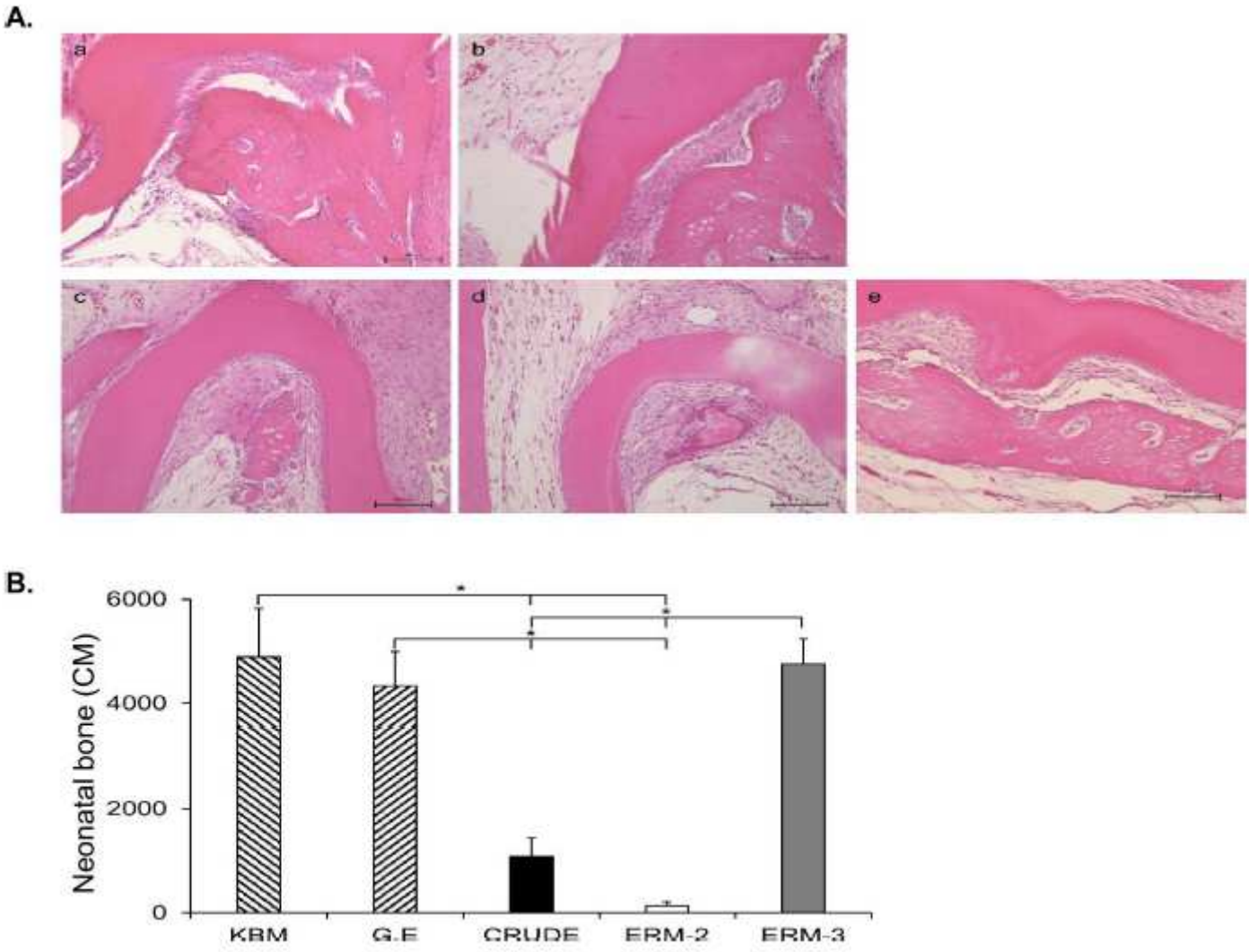

Figure 7

Hematoxylin-eosin (H &E) staining and measurement of newly formed bones in rat mandibular first molar furcation area. A. Micrographs of the bifurcation areas of the roots. a,b. The teeth cultured in control group (fresh KBM and G.E supernatant) demonstrated larger areas of bone formation along with dentoalveolar ankylosis. c, d, e Teeth cultured in supernatants from the CRUDE ERM and ERM-2 cells formed smaller areas of new bone compare to those cultured in ERM-3 cell-derived supernatant; none of the experimental groups developed dentoalveolar ankylosis. Scale bar = 100 μm. B. Bar graph comparing the quantity of bone formation among the various groups (n = 3). The teeth cultured in supernatants derived from the CRUDE ERM and ERM-2 cells (cells with highest levels of amelogenin) demonstrated significantly lower areas of bone formation compared to those cultured in the supernatants derived from ERM-3 cells (lowest level of amelogenin), G.E cells, and KBM. Additionally, teeth cultured in CRUDE ERM cell-derived supernatant demonstrated significantly larger bone formations than those cultured in ERM-2 cell-derived supernatant.

Supplementary Files

This is a list of supplementary files associated with this preprint. Click to download.

- Supplementarydata.pdf